JPEDAV (2015) 36:306–316
DOI: 10.1007/s11669-015-0384-4
1547-7037 ©ASM International

Experimental Investigation of the Phase Relations of the Dy-Mn-As System at 773 K

Z.F. Gu, S.L. Yu, Ch.F. Xu, Z.X. Li, G. Cheng, L. Ma, Y.S. Du, L. Li, M.H. Jiang, and L.Y. Cheng

(Submitted January 7, 2015; in revised form April 7, 2015; published online April 29, 2015)

The isothermal section of the Dy-Mn-As ternary system at 773 K has been investigated by using x-ray diffraction, scanning electron microscopy and energy dispersive spectroscopy. This isothermal section consists of 12 single-phase regions, 21 two-phase regions and 10 three-phase regions. The highest solid solubility of Dy in MnAs is about 0.65 at.%Dy, and that of Mn in DyAs is less than 0.79 at.%Mn. The maximum solubility of As in $DyMn_2$ is less than 0.33 at.%As. No ternary compound was found to exist in this section at 773 K.

Keywords Dy-Mn-As alloy system, phase diagram, SEM observation, X-ray diffraction

1. Introduction

MnAs alloy has been found to have a giant magnetocaloric effect, but it is accompanied with large thermal hysteresis which is unfavorable for practical application in magnetic refrigeration. Thus, many researchers do their best to improve the magnetic refrigeration effect of alloy MnAs by substituting Mn with the third element such as Cr, Al, Cu, Ti and V.[1-4] Dysprosium-based alloys are extensively studied because of their magnetic properties and applications in the magnetic refrigeration field.[5-7] However, the effect of the addition of Dy on magnetic properties of MnAs alloy has not been reported. In order to provide valuable information for developing new materials, the 773 K isothermal section of the Dy-Mn-As system has been constructed in the present work.

The phase diagram of the Dy-Mn binary system is available in literatures.[8-11] It was investigated experimentally by Kirchmayr and Lugscheider using differential thermal analysis,[9] as shown in Fig. 1(a). It is found that there are three phases: the $MgCu_2$-type phase $DyMn_2$, the Th_6Mn_{23}-type phase Dy_6Mn_{23} and the $ThMn_{12}$-type tetragonal phase $DyMn_{12}$.[10]

The assessed Mn-As phase diagram is adopted primarily from Ref 12, which determined the Mn-rich liquidus boundaries, as shown in Fig. 1(b). The As-rich part of this binary phase diagram is still unknown. It includes these following phases: NiAs-type phase γAsMn existing between the congruent melting point at 1208 and 398 K, MnP-type phase βAsMn existing between 398 and 318 K, ferromagnetic NiAs-type phase αAsMn below 318 K, tetragonal phase As_3Mn_4, βAs_2Mn_3 phase, αAs_2Mn_3 phase, tetragonal Cu_2Sb-type phase $AsMn_2$ with a congruent melting point at 1302 K, orthorhombic phase $AsMn_3$.

The phase diagram of the Dy-As system was based primarily on the work of Ref 13, as shown in Fig. 1(c). The NaCl-type phase AsDy has been found. Using a differential calorimetry method, Hanks and Faktor had measured the formation enthalpy of AsDy and the value was up to $\Delta H^S_{AsDy} = -163$ kJ/mol.[14] Crystallographic data on Dy-Mn, Mn-As and Dy-As binary compounds are collected in Table 1.

2. Experimental Procedure

All samples with total masses of about 1.5 g were prepared from highly pure materials (the purity of Mn, Dy and As was 99.95, 99.99 and 99.999 wt.%, respectively).

The samples with less than 10 wt.%As were prepared by arc melting under highly pure argon atmosphere. To compensate for sublimation loss of Mn and As, the extra 3 wt.%Mn and 30 wt.%As were added. The alloy buttons were remelted at least four times to ensure a good homogeneity. During the melting, the melting current should be suitably controlled in order to reduce the loss of As. The mass loss of each sample was kept below 1 wt.%. All the as-cast samples were sealed in quartz tubes pre-evacuated and refilled with purified argon, and then annealed at 773 K for 30 days.

Considering the sublimation of Arsenic at below 900 K in atmospheric pressure, the other samples with more than 10 wt.%As were synthesized by using solid-state diffusion reaction. The starting materials were made into small powders, mixed according to the stoichiometry and compacted into pellets. The prepared pellets wrapped completely in Tantalum foil (in order to reduce the sublimation) were sealed in evacuated quartz tubes and then annealed at 773 K for 5 days, cooled, grinded to powder, pressed into pellets,

Z.F. Gu, S.L. Yu, Z.X. Li, G. Cheng, L. Ma, Y.S. Du, L. Li, M.H. Jiang, and **L.Y. Cheng**, School of Material Science and Engineering, Guilin University of Electronic Technology, Guilin, Guangxi, People's Republic of China; and **Ch.F. Xu**, School of Material Science and Engineering, Guilin University of Electronic Technology, Guilin, Guangxi, P.R. China; and Department of Mechanical Engineering, Guilin University of Aerospace Technology, Guilin 541004 Guangxi, People's Republic of China. Contact e-mail: afu0007@163.com.

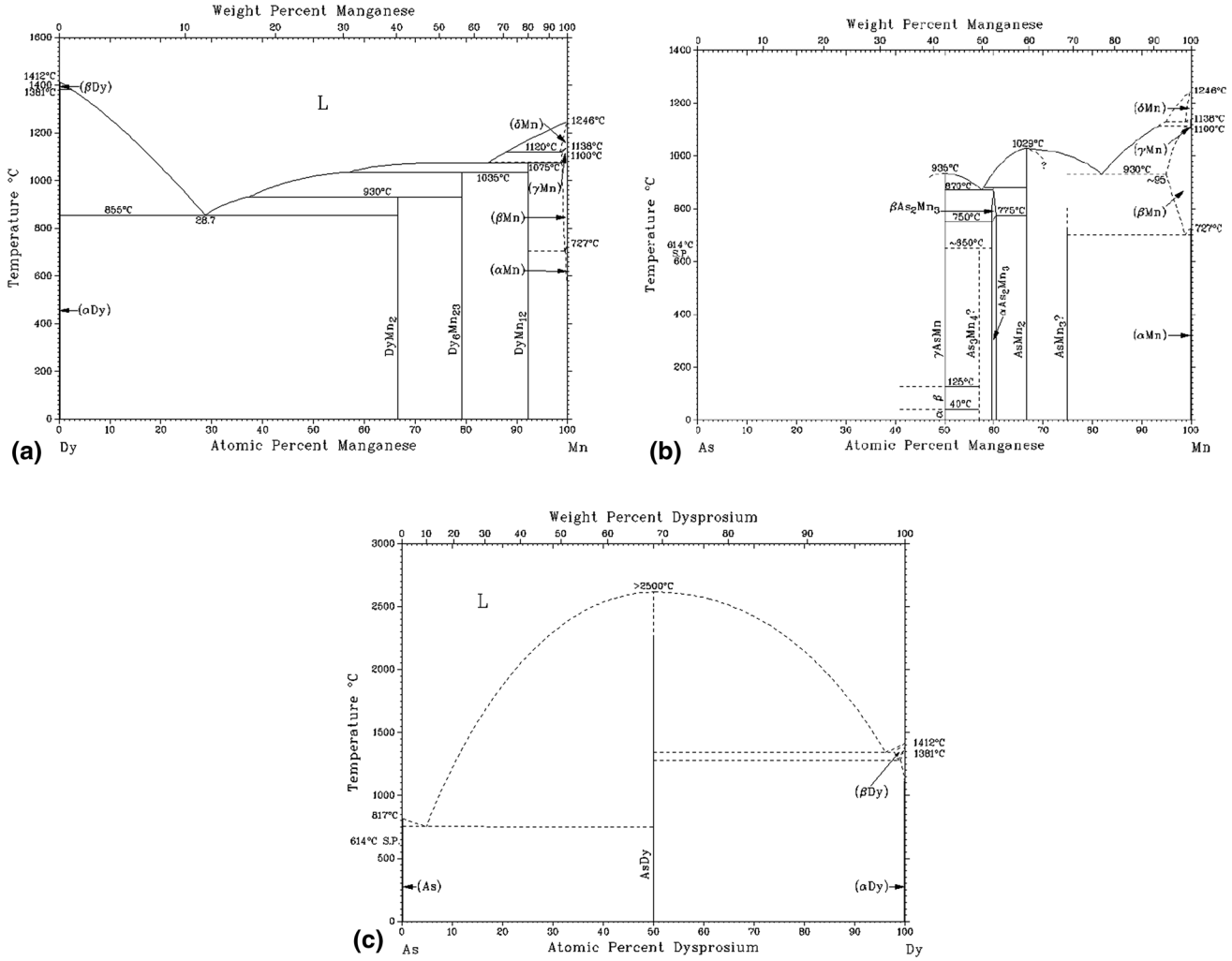

Fig. 1 The binary phase diagrams of Dy-Mn (a), Mn-As (b) and As-Dy (c) from Ref 9,11,12, respectively

Table 1 Crystallographic data of binary compounds in Dy-Mn-As system

Compounds	Space group	Structure type	Lattice parameters, Å			References
			a	*b*	*c*	
$DyMn_2$	*Fd*-3*m*	Cu_2Mg	7.56(1)	…	…	[16]
Dy_6Mn_{23}	*Fm*-3*m*	$Mn_{23}Th_6$	12.358(1)	…	…	[16]
$DyMn_{12}$	I4/*mmm*	$Mn_{12}Th$	8.672(1)	…	4.762(1)	[16]
AsDy	*Fm*-3*m*	NaCl	5.794(1)	…	…	[17]
AsMn	$P6_3/mmc$	NiAs	3.724(1)	…	5.706(1)	[17]
As_3Mn_4	*C*2/*m*	βV_4As_3	13.411(2)	3.693 (1)	9.628(1)	[18]
$AsMn_2$	*P*4/*nmm*	Cu_2Sb	3.769(1)	…	6.278(1)	[17]
$AsMn_3$	*Pmmn*	$AsMn_3$	3.78(1)	3.78(1)	16.26(1)	[17]
αAs_2Mn_3	C2/*m*	…	13.856(2)	3.777(1)	13.622(1)	[19]

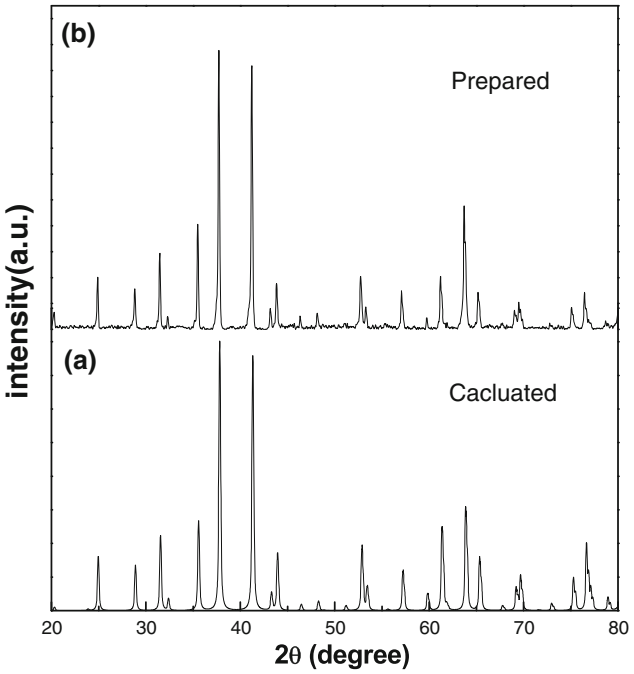

Fig. 2 (a) Calculated pattern for phase Dy_6Mn_{23} from Ref 15; (b) the XRD pattern of alloy Dy_6Mn_{23} annealed at 773 K for 30 days

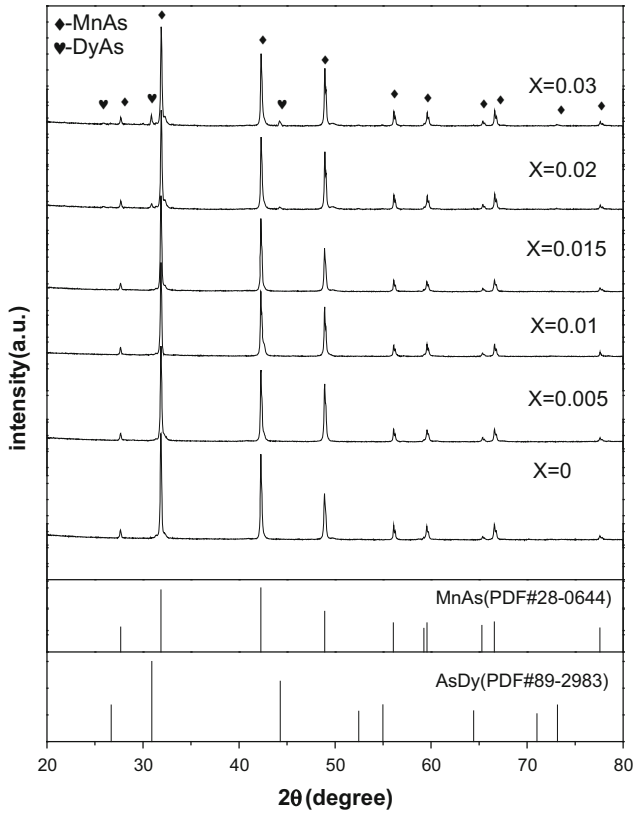

Fig. 3 The XRD patterns of alloys $Mn_{1-x}Dy_xAs$ (x = 0, 0.005, 0.01, 0.015, 0.02, 0.03) annealed at 773 K for 20 days

sealed again and annealed for 15 days to ensure homogeneity. Finally, all ampoules with the samples were quenched into ice water. After the thermal treatment, the mass loss of each sample was also checked and kept below 1 wt.%.

All samples were grinded into powder in acetone to prevent sample oxidation. Powder were sealed again in evacuated quartz tubes and annealed at 773 K for 100 h to eliminate the stress and quenched in water for XRD. Powder XRD analysis was performed from 20° to 80° with a step size of 0.02°. The patterns were analyzed using MDI Jade 6.0 software with the JCPDS-ICDD Powder Diffraction File database. The scanning electron microscopy (SEM) images were from backscattered electrons. A combination of energy dispersive spectroscopy (EDS) phase composition analyses, XRD with Cu Kα radiation (λ = 0.154184 nm), peak matching from patterns of known phases in the JCPDS database, and metallography were used to elucidate the phases present in this study. The Rietveld method was used to determine the lattice parameters of samples by means of the MDI Jade 6 software for XRD pattern processing and the residual R values of less than 9% were considered to be reasonable.

3. Results and Discussion

3.1 Phase Analysis

X-ray diffraction (XRD) analysis of the alloys in these Dy-Mn, Mn-As and As-Dy binary systems confirmed the existence of nine binary compounds at 773 K: $DyMn_2$, Dy_6Mn_{23}, $DyMn_{12}$, γAsMn, As_3Mn_4, αAs_2Mn_3, $AsMn_2$,

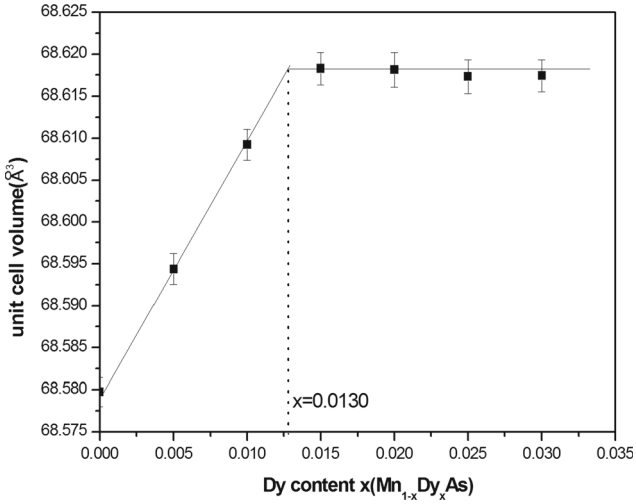

x	Results of EDS analysis (at.%)			Volume (Å^3)	Volume error
	Dy	Mn	As		
0	0	49.98	50.02	68.57972	0.00173
0.005	0.26	49.73	50.01	68.5944	0.00182
0.01	0.52	49.46	50.02	68.60923	0.00186
0.015	0.76	49.21	50.03	68.61828	0.00195
0.02	1	48.99	50.01	68.61813	0.00207
0.03	1.54	48.42	50.04	68.61746	0.00189

Fig. 4 The relationship between unit cell volumes of alloys $Mn_{1-x}Dy_xAs$ (x = 0, 0.005, 0.01, 0.015, 0.02, 0.03) and Dy content x

$AsMn_3$, AsDy, which are good agreement with those reported in Ref 9,11,12. Most of the PDF files of these binary compounds mentioned above are available on JCPDS PDF Cards (2004), except for the Dy_6Mn_{23} compound. The XRD patterns for the Dy_6Mn_{23} compound were calculated from their crystallographic data of Ref 15 by using the PCW 2.3 software. It is found that the calculated results are fully consistent with the experimental XRD patterns of this sample with the nominal composition Dy_6Mn_{23} prepared by arc melting and annealed at 773 K for 30 days, as shown in Fig. 2.

3.2 Solid Solubility

In order to determine the solid solubility of Dy in MnAs, a series of alloys $Dy_xMn_{1-x}As$ (x = 0, 0.005, 0.01, 0.015, 0.02, 0.03) annealed at 773 K for 20 days were prepared, and their XRD results are shown in Fig. 3. A second phase AsDy was observed with Dy content x increasing to 0.02. The corresponding unit cell volumes were calculated by using the Rietveld method in the MDI Jade 6 program. The relationship between the unit cell volume and the Dy content x is displayed by the solid line, as presented in

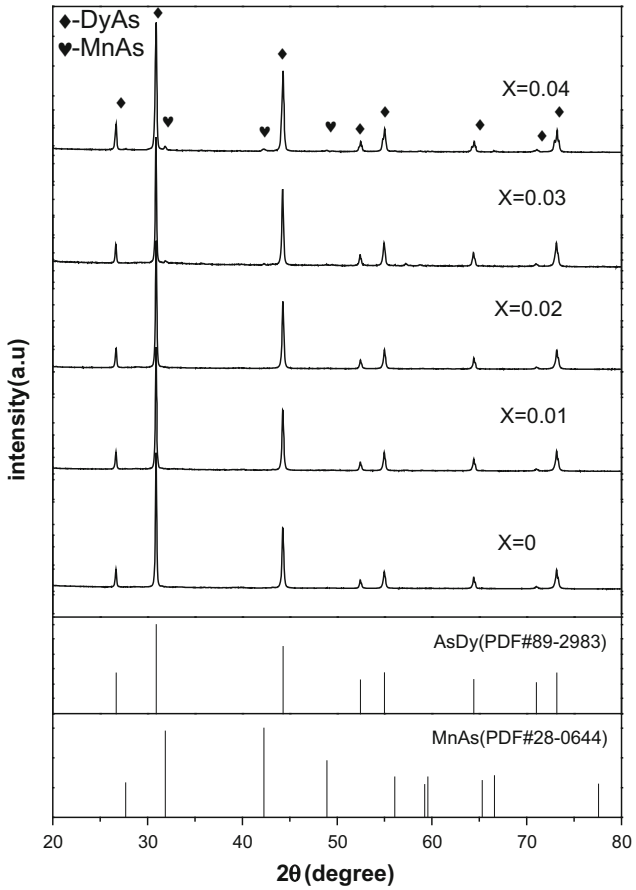

Fig. 5 The XRD patterns of alloys $Mn_xDy_{1-x}As$ (x = 0, 0.01, 0.02, 0.025, 0.03) annealed at 773 K for 20 days

Fig. 4. It shows that the solubility limit of Dy in MnAs is about 0.65 at.%Dy corresponding to the intersection of the two solid lines.

In order to determine the solid solubility of Mn in AsDy, the alloys $Mn_xDy_{1-x}As$ (x = 0, 0.01, 0.02, 0.025, 0.03) annealed at 773 K for 20 days were prepared and their XRD patterns are shown in Fig. 5. A second phase MnAs was observed with Mn content x increasing to 0.025. The corresponding lattice parameters were calculated by using the Rietveld method in the MDI Jade 6 program. The relationship between the lattice parameters and the Mn content x is displayed by the solid line, as presented in Fig. 6. This indicates that the solubility limit of Mn in DyAs is about 0.79 at.%Mn corresponding to the intersection of the two solid lines.

In order to determine the solid solubility of As in $DyMn_2$, the alloys $DyMn_{2(1-x)}As_x$ (x = 0, 0.01, 0.02) annealed at 773 K for 20 days were prepared, and their XRD patterns are shown in Fig. 7. The second phase AsDy was observed with As content x increasing to 0.01. This means that the maximum solubility of As in $DyMn_2$ is less than 0.33 at.%As.

3.3 Dy-Mn-As Ternary System at 773 K

In total, 50 samples in the Dy-Mn-As system were studied by XRD as well as SEM and energy dispersion spectroscopy for some selected characteristic samples to determine the phase compositions.

As far as can be seen from the binary systems, the As-rich side is unknown. Thus, we prepared alloys $Dy_{30}Mn_{10}As_{60}$, $Dy_{20}Mn_{20}As_{60}$, $Dy_{10}Mn_{30}As_{60}$ annealed at 773 K for 20 days in the As-rich corner of the Dy-Mn-As ternary system and their XRD patterns are shown in Fig. 8. One can visualize that all of them are confirmed to be located in the three-phase region: As + AsDy + γAsMn.

The results of XRD and SEM measurements on the $Dy_{50}Mn_{40}As_{10}$ alloy annealed at 773 K for 20 days, which were used to determine the one three-phase region of Dy-Mn-As system, are displayed in Fig. 9. From the XRD data, it can be clearly identified that the alloy $Dy_{50}Mn_{40}As_{10}$ consists of three phases: $DyMn_2$, DyAs and αDy. Meanwhile, the SEM micrograph shown in Fig. 9(b) also

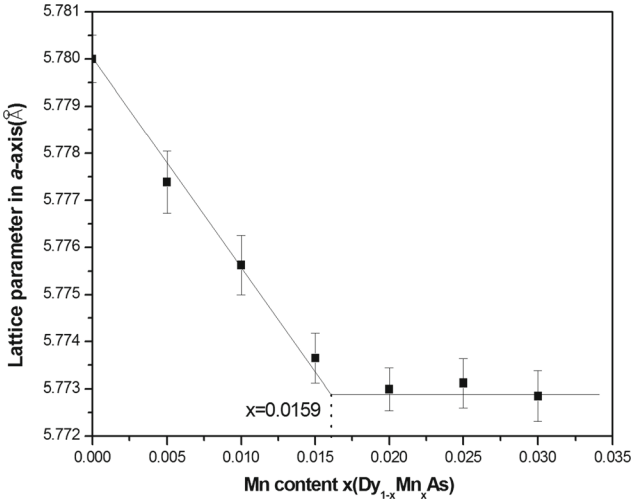

x	Results of EDS analysis (at.%)			a (Å)	a error
	Dy	Mn	As		
0	50.01	0	49.99	5.78	0.00051
0.01	49.49	0.50	50.01	5.77563	0.00063
0.02	48.99	1.01	50	5.77299	0.00045
0.025	48.77	1.27	49.96	5.77312	0.00052
0.03	48.49	1.50	50.01	5.77285	0.00054

Fig. 6 The relationship between lattice parameters of alloys $Dy_{1-x}Mn_xAs$ (x = 0, 0.01, 0.02, 0.025, 0.03) and Mn content x

demonstrates that it includes the same three phases. The similar experimental observation is also found in other alloys. The alloy $Dy_{30}Mn_{60}As_{10}$ is located in the $DyMn_2$, Dy_6Mn_{23} and DyAs three-phase region (see Fig. 10) and the alloy $Dy_{20}Mn_{70}As_{10}$ contains three phases: Dy_6Mn_{23}, $DyMn_{12}$ and DyAs, as illustrated in Fig. 11.

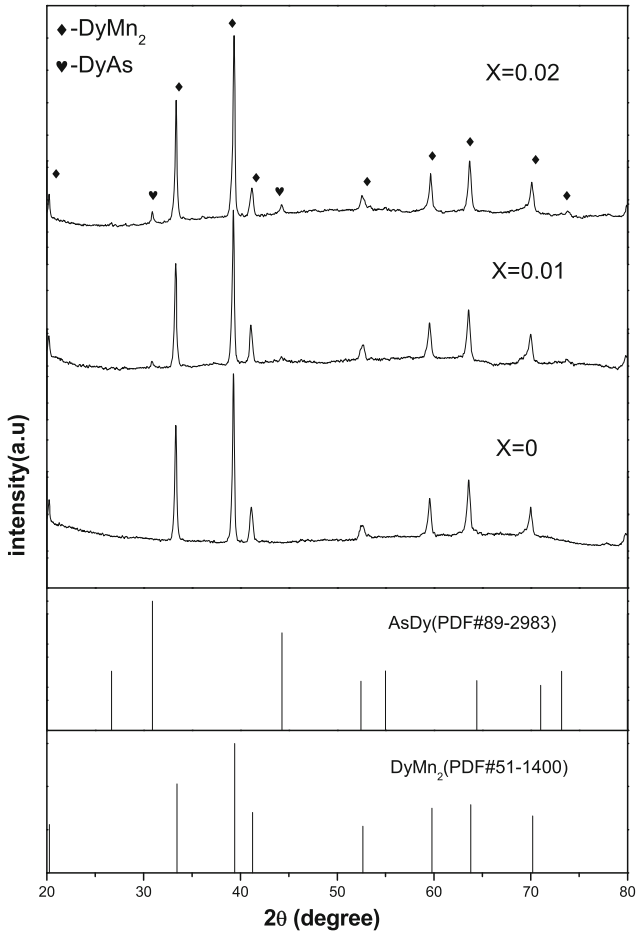

Fig. 7 The XRD patterns of alloys $DyMn_{2(1-x)}As_x$ (x = 0, 0.01, 0.02) annealed at 773 K for 20 days

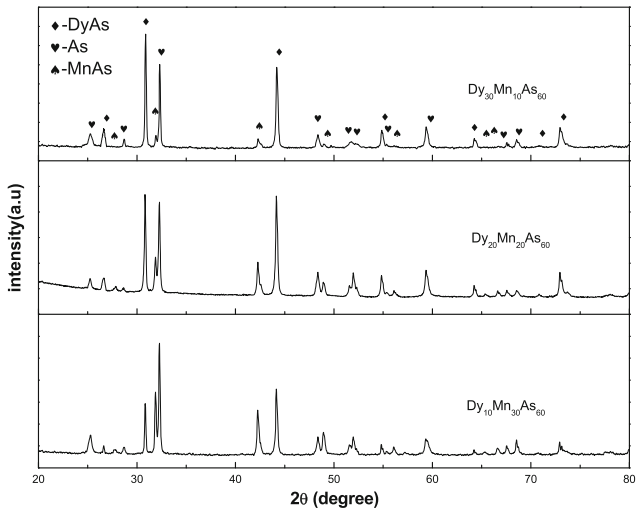

Fig. 8 The XRD patterns of alloys $Dy_{30}Mn_{10}As_{60}$, $Dy_{20}Mn_{20}As_{60}$, $Dy_{10}Mn_{30}As_{60}$ annealed at 773 K for 20 days

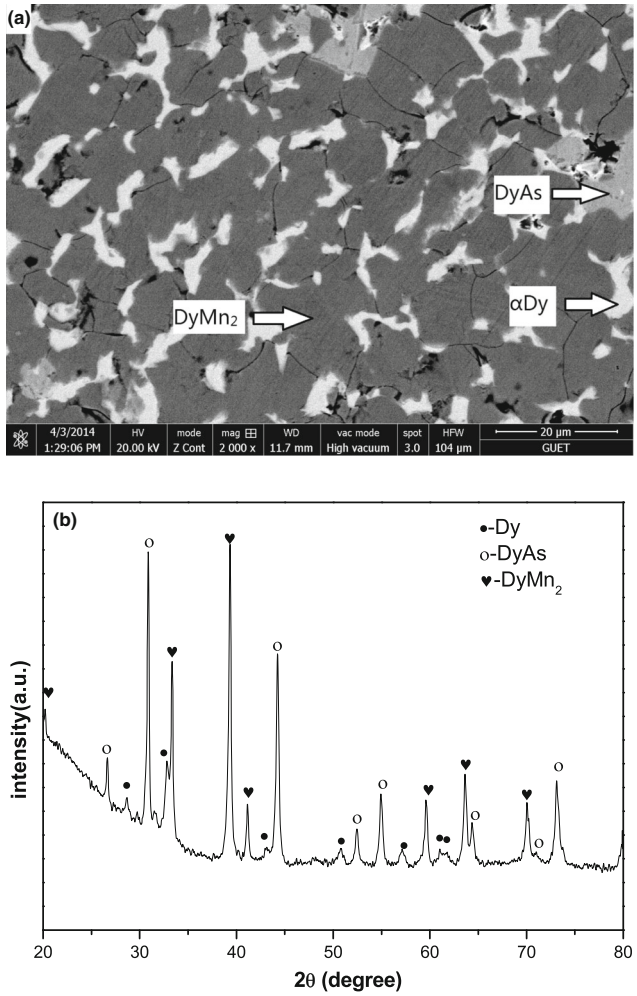

Fig. 9 The SEM micrograph (a) and XRD pattern (b) of the $Dy_{50}Mn_{40}As_{10}$ alloy annealed at 773 K for 20 days

By analyzing the XRD patterns, the $Dy_{10}Mn_{80}As_{10}$ alloy can be identified to include two phases: αMn and DyAs, as shown in Fig. 12, and the alloy $Dy_{10}Mn_{70}As_{20}$ consists of three phases: αMn, DyAs and $AsMn_3$, as presented in Fig. 13. In order to determine one two-phase region, a series of alloys $Dy_{40}Mn_{10}As_{50}$, $Dy_{30}Mn_{20}As_{50}$, $Dy_{20}Mn_{30}As_{50}$ and $Dy_{10}Mn_{40}As_{50}$ were prepared and their XRD patterns are shown in Fig. 14. All of them confirm the existence of the γAsMn and DyAs two-phase region.

Table 2 lists the phase compositions and phase relations of the selected characteristic samples which are crucial to determine the phase boundaries or phase regions. By comparing and analyzing all the results obtained, the isothermal section of the ternary system Dy-Mn-As at 773 K was constructed, as shown in Fig. 15. This section includes 12 single-phase regions, 21 two-phase regions and 10 three-phase regions.

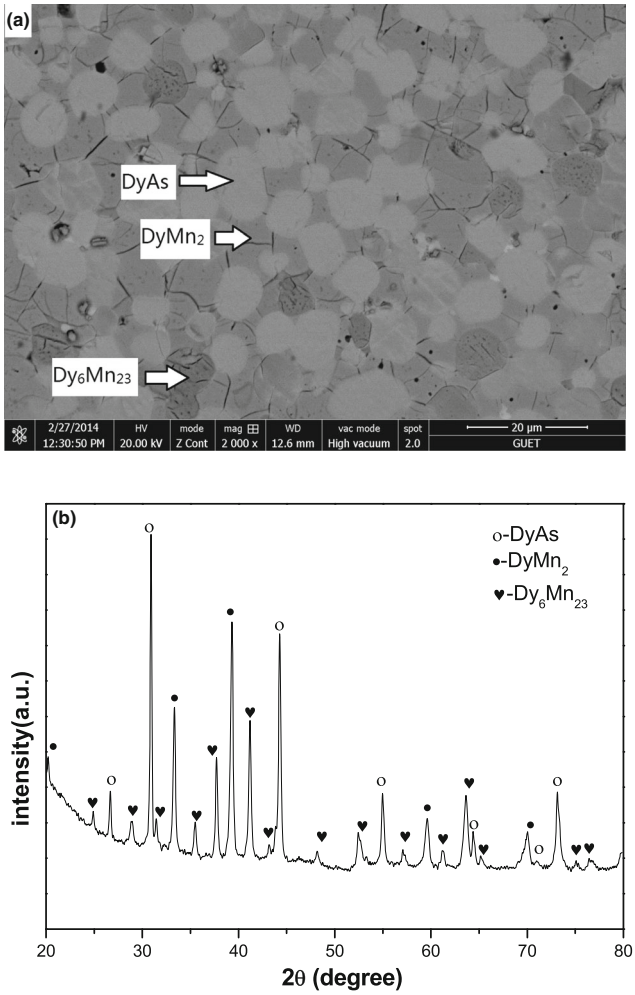

Fig. 10 The SEM micrograph (a) and XRD pattern (b) of the $Dy_{30}Mn_{60}As_{10}$ alloy annealed at 773 K for 20 days

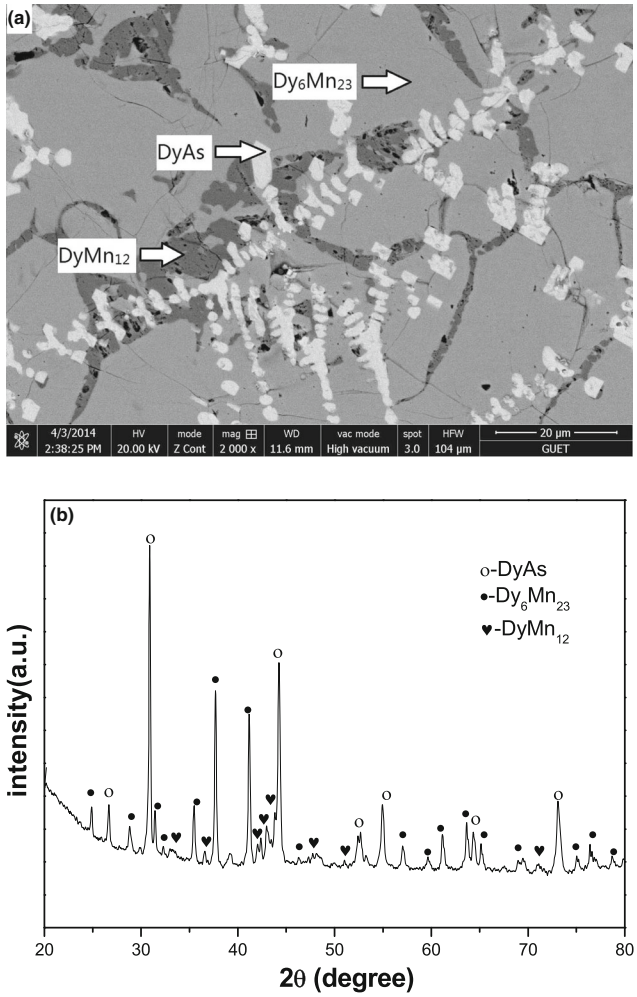

Fig. 11 The SEM micrograph (a) and XRD pattern (b) of the $Dy_{20}Mn_{70}As_{10}$ alloy annealed at 773 K for 20 days

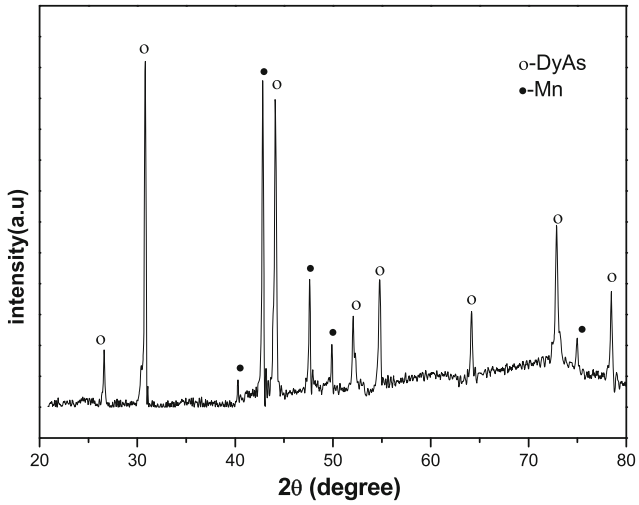

Fig. 12 The XRD pattern of the $Dy_{10}Mn_{80}As_{10}$ alloy annealed at 773 K for 20 days

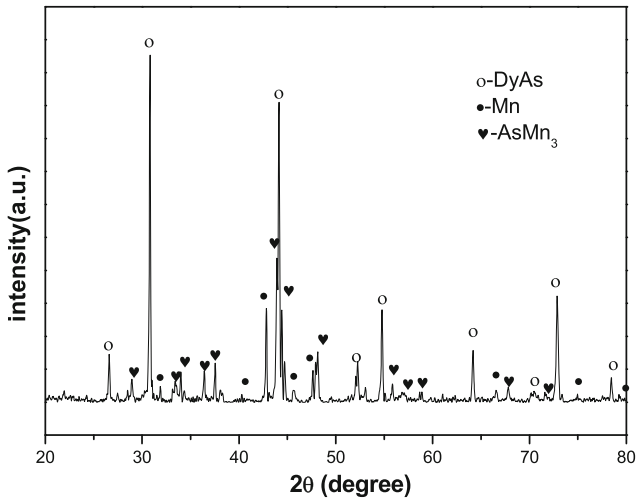

Fig. 13 The XRD pattern of the $Dy_{10}Mn_{70}As_{20}$ alloy annealed at 773 K for 20 days

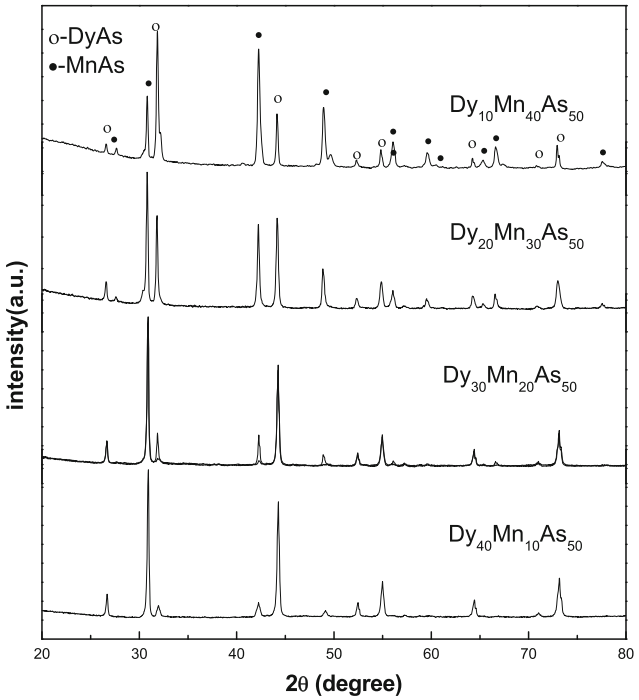

Fig. 14 The XRD patterns of the alloys $Dy_{40}Mn_{10}As_{50}$, $Dy_{30}Mn_{20}As_{50}$, $Dy_{20}Mn_{30}As_{50}$ and $Dy_{10}Mn_{40}As_{50}$ annealed at 773 K for 20 days

Table 2 Phase identification for selected characteristic ternary alloys at 773 K

Alloys	Ternary alloys	Results of EDS analysis, at.%			Phase identified	Lattice parameter, Å		
		Dy	Mn	As		*a*	*b*	*c*
1	$Dy_{70}Mn_{20}As_{10}$	99.11	0.89	0	αDy	3.59457(50)	…	5.65966(55)
		49.02	0.42	50.56	DyAs	5.79053(62)	…	
		33.29	65.61	1.1	$DyMn_2$	7.59432(55)	…	
2	$Dy_{50}Mn_{40}As_{10}$	99.53	0.47	0	αDy	3.58949(63)	…	5.66011(72)
		50.27	0.31	49.42	DyAs	5.78442(66)	…	…
		32.91	66.34	0.75	$DyMn_2$	7.59289(57)	…	…
3	$Dy_{30}Mn_{60}As_{10}$	33.37	65.86	0.77	$DyMn_2$	7.59010(62)	…	…
		20.24	79.5	0.26	Dy_6Mn_{23}	12.39157(97)	…	…
		49.48	0.67	49.85	DyAs	5.78273(66)	…	…
4	$Dy_{20}Mn_{70}As_{10}$	18.2	2.97	78.83	Dy_6Mn_{23}	12.39213(93)	…	…
		49.02	0.42	50.56	DyAs	5.78342(57)	…	…
		7.25	92.54	0.21	$DyMn_{12}$	8.59268(77)	…	4.76395(83)
5	$Dy_{13}Mn_{77}As_{10}$	0	99.91	0.09	αMn	8.93162(79)	…	…
		7.33	92.39	0.28	$DyMn_{12}$	8.58568(71)	…	4.75712(78)
		48.2	2.52	49.28	DyAs	5.77871(64)	…	…
6	$Dy_{10}Mn_{80}As_{10}$	…	…	…	αMn	8.93541(73)	…	…
		…	…	…	DyAs	5.79058(56)	…	…
7	$Dy_{10}Mn_{70}As_{20}$	…	…	…	αMn	8.92124(73)	…	…
		…	…	…	DyAs	5.80146(57)	…	…
		…	…	…	$AsMn_3$	3.78020(34)	3.79356(39)	16.29793(113)
8	$Dy_{10}Mn_{57}As_{33}$	…	…	…	DyAs	5.79373(61)	…	…
		…	…	…	$AsMn_3$	3.77804(41)	3.78539(46)	16.33494(124)
		…	…	…	$AsMn_2$	3.78643(37)	…	6.26683(67)
9	$Dy_{10}Mn_{51}As_{39}$	…	…	…	DyAs	5.7849(49)	…	…
		…	…	…	$AsMn_2$	3.78459(32)	…	6.24412(57)
		…	…	…	αAs_2Mn_3	13.27093(95)	3.69132(33)	13.6323(96)
10	$Dy_{10}Mn_{47}As_{43}$	…	…	…	DyAs	5.78016(56)	…	…
		…	…	…	αAs_2Mn_3	13.25016(98)	3.69501(39)	13.6611(101)
		…	…	…	As_3Mn_4	13.40779(99)	3.69544(37)	9.62326(83)
11	$Dy_{10}Mn_{43}As_{47}$	…	…	…	DyAs	5.79586(63)	…	…
		…	…	…	As_3Mn_4	13.42994(96)	3.68107(31)	9.62455(79)
		…	…	…	γAsMn	3.71972(32)	…	5.71395(53)
12	$Dy_{40}Mn_{10}As_{50}$	…	…	…	DyAs	5.77844(59)	…	…
		…	…	…	γAsMn	3.7075(38)	…	5.68817(57)
13	$Dy_{30}Mn_{20}As_{50}$	…	…	…	DyAs	5.78295(62)	…	…
		…	…	…	γAsMn	3.72236(36)	…	5.70256(63)
14	$Dy_{20}Mn_{30}As_{50}$	…	…	…	DyAs	5.78271(60)	…	…
		…	…	…	γAsMn	3.71554(34)	…	5.70567(55)
15	$Dy_{10}Mn_{40}As_{50}$	…	…	…	DyAs	5.79011(53)	…	…
		…	…	…	γAsMn	3.71893(32)	…	5.70579(53)
16	$Dy_{30}Mn_{10}As_{60}$	…	…	…	DyAs	5.79353(66)	…	…
		…	…	…	γAsMn	5.79307(66)	3.6326(35)	6.36997(67)
		…	…	…	As	3.75912(32)	…	10.54882(87)
17	$Dy_{20}Mn_{20}As_{60}$	…	…	…	DyAs	5.79672(56)	…	…
		…	…	…	γAsMn	3.72396(33)	…	5.70299(57)
		…	…	…	As	3.76252(39)	…	10.55051(91)
18	$Dy_{10}Mn_{30}As_{60}$	…	…	…	DyAs	5.79574(61)	…	…
		…	…	…	γAsMn	3.72018(38)	…	5.70874(59)
		…	…	…	As	3.76147(36)	…	10.55083(88)

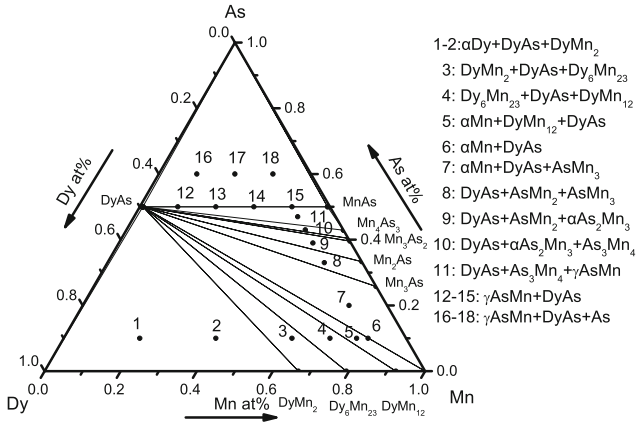

Fig. 15 The isothermal section of the Dy-Mn-As ternary phase diagram at 773 K

4. Conclusion

This isothermal section of the Dy-Mn-As ternary system at 773 K consists of 12 single-phase regions, 21 two-phase regions and 10 three-phase regions. No ternary compound was found to exist in this section at 773 K. The highest solid solubility of Dy in MnAs is about 0.65 at.%Dy, and that of Mn in DyAs is less than 0.79 at.%Mn. The maximum solubility of As in $DyMn_2$ is less than 0.33 at%As.

Acknowledgments

This work was supported by the National Natural Science Foundation of China (Grant Nos. 50261002, 50661002 and 51161005) and National Basic Research Program of China (No. 2014CB643703).

References

1. N.K. Sun, W.B. Cui, D. Li, D.Y. Geng, F. Yang, and Z.D. Zhang, Giant Room-Temperature Magnetocaloric Effect in $Mn_{1-x}Cr_xAs$, *Appl. Phys. Lett.*, 2008, **92**(7), p 072504
2. W.B. Cui, W. Liu, X.H. Liu, S. Guo, Z. Han, X.G. Zhao, and Z.D. Zhang, Beneficial Effect of Minor Al Substitution on the Magnetocaloric Effect of $Mn_{1-x}Al_xAs$, *Mater. Lett.*, 2009, **63**(6), p 595-597
3. D.L. Rocco, A. de Campos, A.M.G. Carvalho, L. Caron, A.A. Coelho, S. Gama et al., Ambient Pressure Colossal Magnetocaloric Effect in $Mn_{1-x}Cu_xAs$ Compounds, *Appl. Phys. Lett.*, 2007, **90**(24), p 242507
4. M. Balli, D. Fruchart, D. Gignoux, C. Dupuis, A. Kedous-Lebouc, and R. Zach, Giant Magnetocaloric Effect in $Mn_{1-x}(Ti0.5V0.5)_xAs$: Experiments and Calculations, *J. Appl. Phys.*, 2008, **103**(10), p 103908
5. X.X. Zhang, F.W. Wang, and G.H. Wen, Magnetic Entropy Change in RCoAl (R = Gd, Tb, Dy, and Ho) Compounds: Candidate Materials for Providing Magnetic Refrigeration in the Temperature Range 10 K to 100 K, *J. Phys. Condens. Matter*, 2001, **13**(31), p L747
6. K.A. Gschneidner, Jr., and V.K. Pecharsky, Rare Earths and Magnetic Refrigeration, *J. Rare Earths*, 2006, **24**(6), p 641-647
7. A.K. Pathak, I. Dubenko, S. Stadler, and N. Ali, Magnetic, Magnetocaloric, and Magnetotransport Properties of $RCo_{1.8}Mn_{0.2}$ (R = Er, Ho, Dy, and Tb) Compounds, *J. Magn. Magn. Mater.*, 2011, **323**(20), p 2436-2440
8. H. Landolt and R. Börnstein, *Phase Equilibria, Crystallographic and Thermodynamic Data of Binary Alloys*, Vol 3, Springer, Berlin, 1993
9. H.R. Kirchmayr and W. Lugscheider, Constitution of Binary Alloys of Gadolinium, Dysprosium, Holmium, and Erbium with Manganese, *Z. Metallkd.*, 1967, **58**, p 185
10. H. Okamoto, Dy-Mn (Dysprosium-Manganese), *J. Phase Equilib. Diffus.*, 2011, **32**, p 167
11. H. Okamoto and T.B. Massalski, Binary Alloy Phase Diagrams Requiring Further Studies, *J. Phase Equilib.*, 1994, **15**(5), p 500
12. M. Hansen and K. Anderko, *Constitution of Binary Alloys*, McGraw-Hill, New York, 1958
13. K.A. Gschneidner, Jr., and F.W. Calderwood, The Arsenic-Rare Earth Systems, *Bull. Alloy Phase Diagr.*, 1986, **7**, p 277
14. R. Hanks and M.M. Faktor, Quantitative Application of Dynamic Differential Calorimetry. Part 2—Heats of Formation of the Group 3 A Arsenides, *Trans. Faraday Soc.*, 1967, **63**, p 1130
15. Pierre Villars and Lauriston D. Calvert, *Pearson's Handbook of Crystallographic Data for Intermetallic Phases*, Vol 2, American Society for Metals, Metals Park, OH, 1985
16. P. Villars, *Pearson's Handbook Desk Edition: Crystallographic Data for Intermetallic Phases*, ASM International, Materials Park, OH, 1997
17. H. Landolt and R. Börnstein, *Phase Equilibria, Crystallographic and Thermodynamic Data of Binary Alloys*, Springer, Berlin, 1993
18. M.F. Hagedorn and W. Jeitschko, Synthesis and Crystal Structure of Mn_4As_3 and Its Relation to Other Manganese Arsenides, *J. Solid State Chem.*, 1995, **119**(2), p 344-348
19. L.Θ. Dietrich, W. Jeitschko, and M.H. Möller, The Crystal Structure of Mn_3As_2 (I), *Cryst. Mater.*, 1989, **190**(1-4), p 259-270